Hydrogel droplet single-cell processing: DNA purification, handling, release, and on-chip linearization

Philip Zimny,[1,2] David Juncker,[1,2,a)] and Walter Reisner[3,a)]
[1]*Department of Biological Engineering, McGill University, Montreal, Quebec H3A 2B4, Canada*
[2]*McGill University and Genome Quebec Innovation Center, 740 Dr. Penfield Avenue, Room 7104, Montreal, Quebec H3A 0G1, Canada*
[3]*Department of Physics, McGill University, 3600 Rue University, Montreal, Quebec H3A 2T8, Canada*

(Received 23 December 2017; accepted 20 February 2018; published online 14 March 2018)

The preparation and handling of mammalian single-cell genomic DNA is limited by the complexity bottleneck inherent to performing multi-step, multi-reagent operations in a microfluidic environment. We have developed a method for benchtop preparation of high-molecular weight, intact, single-cell genomes and demonstrate the extraction of long nucleic acid molecules in a microfluidic system. Lymphoblasts are encapsulated inside of alginate microparticles using a droplet microfluidics, and cells are lysed in bulk. The purified genomes are then delivered to and imaged on a dedicated microfluidic device. High-molecular weight DNA is protected from shear and retains its original cellular identity. Using this encapsulation protocol, we were able to extract individual nucleic acid strands on the millimeter scale inside of a microfluidic channel. *Published by AIP Publishing*. https://doi.org/10.1063/1.5020571

I. INTRODUCTION

Preparation of single-cell genomes has been of mounting interest in the fields of genomics, cellular biology, oncology, and reproductive medicine. Studies of individual cells provide for a more granular understanding of gene function by removing averaging bias present in data collected from ensemble samples.[1] Single-cell data may be useful for investigating unique clonal subpopulations present within the same tumour, termed intra-tumour heterogeneity.[2–5] The underlying genomic "profiles" of these distinct subpopulations can be informative for prognostic indicators like potential for metastasis, susceptibility to treatment, and patient survivability.[6] In some cancers, metastatic cells which traverse a patient's bloodstream, called circulating tumour cells (CTCs), are believed to have prognostic value in predicting survival. They also offer a less invasive alternative to solid biopsies and promise higher frequency sampling to generate dynamic disease models.[7] Preimplantation screening of individual embryos is a common practice prior to *in vitro* fertilization and relies on small sample sizes (one or two cells).[8]

Next-Generation Sequencing (NGS) is the dominant technology for investigating single-cell genomes. However, automated microfluidic platforms tailored to producing single-cell DNA for NGS often result in a considerable degree of DNA fragmentation.[9–14] This is a significant drawback, as platforms for single-cell, single-molecule genomic analysis have emerged that require samples consisting of long nucleic acids (0.1–1 Mbp). Working with longer nucleic acids can help resolve systemic NGS errors arising from incomplete coverage, copy number variations (CNVs), and C/G enrichment and help avoid errors arising from DNA amplification (such as allelic dropout (ADO) and preferential amplification of certain sequences).[15,16] High-molecular weight DNA extraction is limited by being relatively low throughput, in part due to the necessity of careful manipulation that ensures that long molecules are not sheared. Such techniques have previously been demonstrated by either using low flow rates during sample preparation performed

[a)]Authors to whom correspondence should be addressed: david.juncker@mcgill.ca, reisner@physics.mcgill.ca

inside a microfluidic cell,[17] or by lysing cells in dead volume chambers before transferring the DNA strands to a central channel for extension.[18] In addition, specialized fluidic devices relying on induced confinement have been used to trap and manipulate long DNA fragments extracted from single mammalian cells inside nanochannel arrays.[19] However, this method did not address the need for simplifying multi-step operations or device contamination with cellular debris.

High-molecular weight, intact nucleic acids, and adequate stretching are necessary for reliable optical mapping of single cell genomes. Usage of long nucleic acids is ideal, since they minimize additional computations required for aligning experimental data to reference genomes. High-molecular weight, single-molecule nucleic acids have traditionally been linearized either using surface immobilization,[20] or trapped and extended inside of microfluidic systems using a number of configurations: optical tweezers,[21] flow or electrophoretic stretching,[22] or nanoconfinement.[23] Most studies have used either purified nucleic acids or reconstituted chromatin. Lambda phage (48 kbp), BAC (>150 kbp) and yeast chromosomal DNA (12.1 Mbp) are common model systems. The largest linearized nucleic acid fragments extracted from eukaryotes as of the writing of this manuscript have been reported to be a 5.7 Mbp (1 mm) section of a *Schizosaccharomyces pombe* chromosome,[24] and over 10 mm using the M0–91 cell line.[17] Few studies have reported single-molecule extraction and visualization directly from single-cells, although usage of dynamic confinement using convex geometries proved fruitful for extracting and extending DNA with a maximum length of 62 μm ($\sim$250 kbp).[19] This constitutes a key milestone for sample preparation integration with optical mapping of single cell genomes.

Hydrogel encapsulation protocols for isolating genomic contents present a unique opportunity to resolve many of the challenges inherent to single-cell sample preparation. Mammalian cells are capable of being encapsulated in hydrogel microspheres and kept viable for a number of days, establishing that molecules essential for cell vitality are capable of diffusing through the hydrogel.[25,26] Biochemical reactions, like an abridged polymerase chain reaction (PCR) protocol for whole genome amplification (WGA), were completed on single-cells trapped inside these microspheres.[27] The microspheres are capable of being generated easily in large numbers using a Na-alginate precursor with a simple crosslinking reaction using established droplet microfluidics systems, and are therefore an ideal candidate system for preparing high molecular weight single-cell genomes. Alginate polymerization and depolymerisation is quickly catalyzed and unaffected by temperature, making it suitable to withstand sample preparation protocols outside of room temperature. Hydrogel spheres have the potential to carry encapsulated, concentrated genomes that are easily manipulated both by pipettes and via microfluidics.

Here, we propose an assay agnostic single-cell sample preparation technique based on alginate microparticle (AMP) encapsulation that enables sample handling and lysis of individual lymphoblast cells using traditional benchtop protocols and visualization of the purified DNA inside of a dedicated microfluidic device. Encapsulation of single human lymphoblasts inside of alginate hydrogels is implemented using water-in-oil droplet microfluidics on a polydimethylsiloxane (PDMS) device [Fig. 1(a)]. The AMPs are added into a bulk solution for cell lysis [Fig. 1(b)] followed by introduction of the processed cells onto a microfluidic device for inspection. AMPs are porous and allow for diffusion of reagents and "waste" molecules into and out the hydrogel matrix; however, chromosomal-length nucleic acids have a radius of gyration significantly larger than the AMP pore size, facilitating effective molecular isolation. Encapsulated chromosomal fragments are protected from shear forces during typical pipetting operations and can be introduced onto a microfluidic device largely intact [Fig. 1(c)]. Operations on the device are powered by syringe-driven hydraulic flow, enabling AMPs to be selected for and captured [Fig. 1(d)] inside a specialized trapping region. Alginate depolymerization [Fig. 1(e)], transfer of the nucleic acids to a shallow microfluidic channel, and fluorescent visualization follow in subsequent operations [Fig. 1(f)].

II. MATERIALS AND METHODS

A. Fabrication of DNA extension devices

In order to fabricate microfluidic devices for DNA extension, we used wafer-scale microfabrication processes [Fig. 2(a)]. Starting substrates were 4″ diameter P-type, single-side

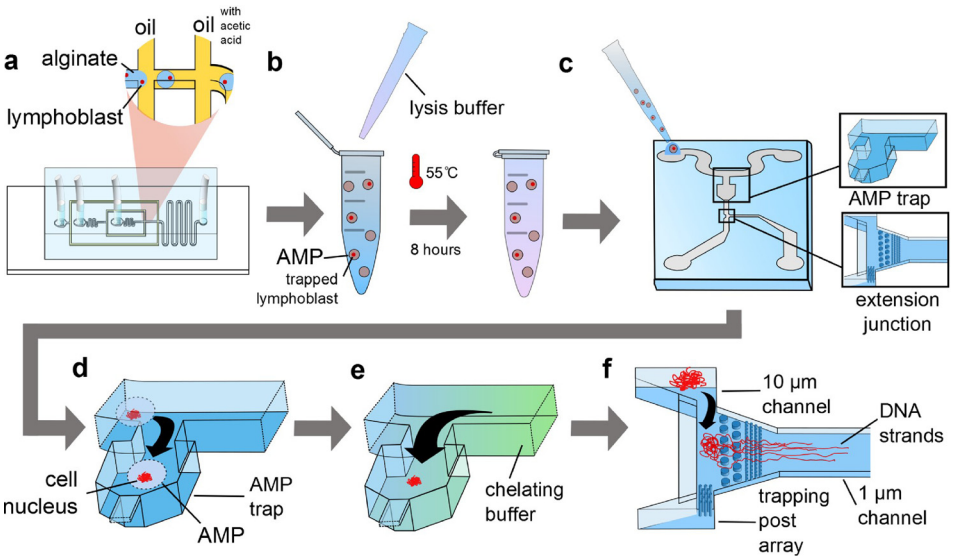

FIG. 1. Workflow of the hydrogel droplet, single-cell processing (HDSCP) using water-in-oil droplet microfluidics, followed by chemical lysis inside of an Eppendorf tube, and extraction and visualization inside of a microfluidic device. (a) Freshly harvested lymphoblasts are encapsulated using a water-in-oil droplet generator. A secondary oil channel contains acetic acid which gelates the droplets into alginate microparticles (AMPs). Individual human lymphoblast cells have been drawn as red dots, while AMPs are grey circles. (b) The AMPs are extracted from the PDMS device into a bulk solution inside a centrifuge tube. Genomic DNA is purified using a lysis protocol in bulk. Individual genomes remain encapsulated inside of the AMPs. (c) The AMPs containing individual genomes are then transferred by a pipette onto a second microfluidic device. Key features of the alginate extractor chip are highlighted: an AMP trapping region (top right), and a genome extraction region (bottom right). (d) Suction induced by a syringe is used to isolate individual AMPs containing lymphoblast genomes inside a dedicated trapping zone. (e) A chelating buffer introduced along the opposite path depolymerizes the hydrogel containing the isolated genome. (f) Purified lymphoblast genomic DNA is drawn into the 10 μm-deep channel before being captured in the post array located at the junction of 10 μm and 1 μm-deep channels. Trapped genomes are then extended by applying a negative pressure bias towards the exhaust port located at the end of 1 μm channel. A post array facilitates efficient separation of entangled nucleic acid strands as the DNA enters the channel.

polished silicon wafers (University Wafer, South Boston, MA, USA). The first step is to use photolithography to pattern the 1 μm-deep extension channel. The wafer was then coated with a 3 μm layer of SiO_2 deposited using plasma-enhanced chemical vapor deposition (PECVD); this layer is used to mask both the 250 μm and 10 μm-deep features. We avoid using separate masking layers for the 250 μm and 10 μm-deep features due to the difficulty of spin coating on the extreme topography created by the 250 μm deep etch. Next, the 250 μm-deep layer (including the AMP trap) [Fig. 2(b)] is formed using deep reactive-ion etching (DRIE). This DRIE step typically consumed about 1–1.5 μm of the SiO_2 layer. The remaining SiO_2 layer was then selectively removed using a dry etch to form the masking pattern for the subsequent DRIE step. A second, shorter DRIE process then etched away 10 μm of silicon to form the feeder channel, including the necessary genome trap and post array [Fig. 2(c)], in addition to the 250 μm channel. The next step requires a backside process; therefore, the topside was covered with SiO_2 to protect it from abrasion. A photolithography process was used to pattern via holes to introduce fluid into the device and connect the device to an external pump. Again, SiO_2 was used as the masking material and the via etch was performed using DRIE. A dicing step was necessary to divide the wafer into tetrads of dimensions 20×20 mm prior to the bonding step. Following an HF dip and piranha clean, the ultraclean tetrads were bonded to borosilicate coverslips (Fisher Scientific, Hampton, NH) diced into 20×20 mm squares. Anodic bonding was used to fully anneal the two materials. Lastly, the tetrads were diced into four individual devices [Fig. 2(d)].

B. Fabrication of droplet generator devices using 3D-printed molds

We first prepared molds for the droplet generator devices fabricated from UV-curable resin using digital light processing (DLP) 3D printing (Envisiontec, Germany). 3D-printed

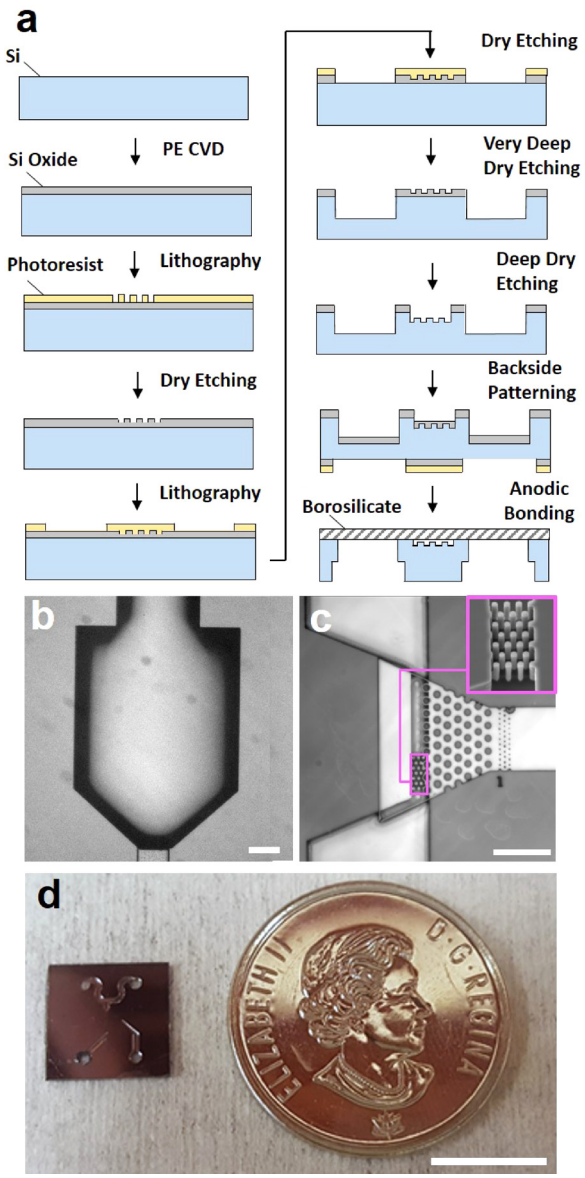

FIG. 2. Microfluidic DNA linearization device fabrication and features. (a) The microfabrication protocol for producing the alginate extractor chip required partial etching of a single SiO layer between the 250 μm and 10 μm-deep etch. A through-etch was performed on the backside due to spincoating limitations on deep features, and borosilicate coverslips were bonded to the chips via anodic bonding. (c) A brightfield image of the AMP trap. (d) A brightfield image of the nucleus trap. Inset: SEM image of the post array for trapping isolated nuclei. (e) Alginate extractor chip displayed with the Canadian quarter for scaling. Scale bars are 100 μm, 50 μm and 1 cm, respectively.

molds have the advantage of a quick production cycle (lasting on the order of several hours) as compared to photolithography, which can take several days due to the necessity of ordering masks and more required labor during the fabrication process. Sylgard 184 (Dow Corning, NY, USA) was mixed according to the manufacturer's instructions using a ratio of 10:1 of base to the curing agent. The mixed PDMS was then poured onto the molds, which were placed on a Petri dish, following a pretreatment with a silicone-based lubricating agent (Mann Release Technologies, Macungie, PA, USA). The Petri dishes were degassed for one hour and then placed in an oven at 60 °C for 8 h to cure. A 0.8 μm micropunch (Ted Pella, Redding, CA, USA) was used to produce access ports in the functioning PDMS replicas. The replicas were then bonded to glass microscope slides (Corning, NY, USA) after 45 s of plasma

treatment (Plasma Preen, North Brunswick, NJ, USA). To ensure satisfactory bonding, the PDMS replicas were clamped to the microscope slides and heated inside an oven at 70 °C for 1 h. Corn oil was to be introduced into the devices; therefore, the channels required sufficient hydrophobicity. The channels were silanized with a solution of 0.1 ml (Tridecafluoro-1,1,2,2-Tetrahydrooctyl)Trichlorosilane in 1.4 ml methanol according to Takeuchi[28] and left to evaporate inside a fume hood. A finished droplet generator is pictured in Fig. 3(a).

C. Alginate microparticle preparation

Although several hydrogels are suitable for transporting cells, alginate was chosen for its relatively quick gelation, stability at higher temperatures, and simple release chemistry. Na-alginate from brown algae (Sigma Aldrich, Oakville, ON, Canada) was dissolved in deionized water to produce 2% (w/w) of which 2 ml was mixed with 20 μl of 2 M $CaCO_3$ nanoparticle solution and 50 μl of concentrated lymphoblast suspension yielding a final product of ~2% alginate, 20 μM $CaCO_3$, 720 cells/ml. The chosen gelation strategy would require the suspended $CaCO_3$ nanoparticles be dissolved via a sudden pH drop initiated by the introduction of acetic acid. Droplet generator devices were connected via luer tubing to 1000 μl glass syringes containing alginate solution, corn oil containing 1% Span 80 (w/w) (Sigma Aldrich, Oakville, ON, Canada), and corn oil with 1% Span 80 and 0.1% glacial acetic acid (Sigma Aldrich, Missouri, USA). A programmable syringe pump (Cetoni NeMESYS, Germany) was set to deliver the liquids at a rate of 0.05 μl/s, 0.2 μl/s, and 0.2 μl/s, respectively. Once fully gelated, alginate microparticles (AMPs) were deposited into a bath of extraction buffer (0.03% TBS, 0.05% Tween 20, 0.1% $CaCl_2$, 0.5% bovine serum albumin) in a centrifuge tube by a short section of tubing. The contents are vortexed to create a water/oil emulsion, and then centrifuged at 1000 rpm for 10 min. Excess oil is aspirated by a pipette, followed by the addition of an excess extraction buffer and a repetition of the centrifugation step. Any remaining oil is aspirated and the AMPs are collected using a wide tip pipette and transferred to a fresh tube.

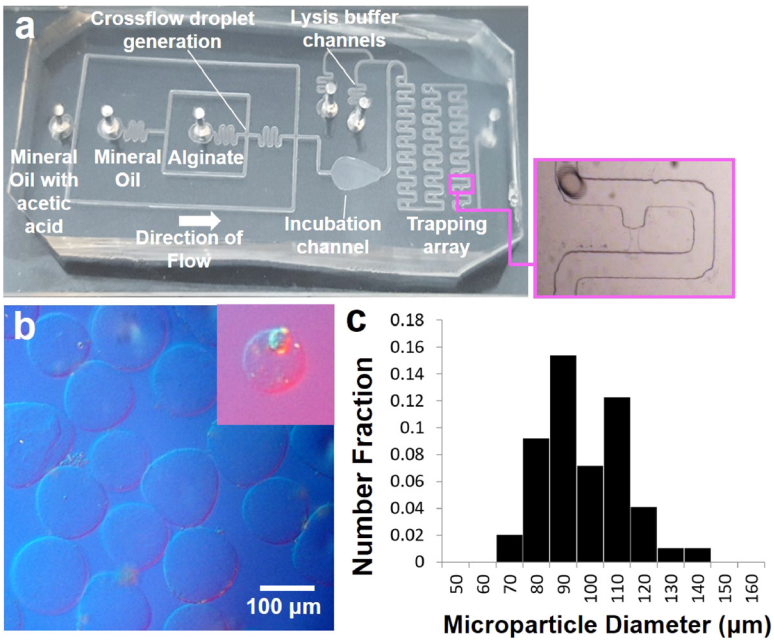

FIG. 3. Droplet generator and alginate microparticles produced using droplet microfluidics. (a) A PDMS droplet generator device which includes a downstream trapping array for closer inspection of lymphoblast-laden microparticles. Additional channels were added to flow lysis buffer into this region in order to validate the in-AMP lysis protocol. Inset: A magnified view of a single trap. (b) A representative sample of alginate microparticles (AMPs) imaged using DIC microscopy. Inset: AMP containing a single lymphoblast cell. (c) Histogram of the AMP diameter for a typical sample.

D. Mammalian cell lysis and genome purification

Cell lysis buffer comprised 0.1% sodium dodecyl sulfate (SDS), 0.1% CHAPS, 150 mM NaCl, 5 mM $CaCl_2$, and 1 mg/ml Proteinase K. A volume of 1.4 ml of cell lysis buffer is added to 100 μl of concentrated AMPs, followed by 0.1 μl of 5 mM SYTO 24 fluorescent dye (Thermofisher Scientific, United States). The centrifuge tubes were thoroughly vortexed, and then immersed in a water bath set to 55 °C for 2–8 h away from light. Vortexing was repeated once after 1 h had passed.

E. Operating DNA extension devices

In order to be operated manually, the microfluidic DNA extraction devices were assembled onto a poly(methyl methacrylate) (PMMA) chuck using 1.5 mm anodized screws and a retaining ring. Luer connectors interfaced the input/output ports on the microfluidic chip to a set of syringe pumps which were used to actuate the fluid inside the device using both hydrostatic and pressure-driven modes. The complete assembly is mounted onto an inverted fluorescence microscope (Nikon, Tokyo, Japan). AMPs were loaded into one of the loading ports in the chuck using a thin tip pipette, and then all loading ports are sealed with nylon screws. A pressure bias was introduced by opening the respective air valves and elevating one valve with respect to the other. AMPs with encapsulated cells were visualized by exciting the SYTO 24 strain with the 488 nm line and captured using negative pressure introduced via the 100 μm-deep channel. Excess AMPs were then flushed by reversing the direction of hydrostatic pressure bias. A chelating buffer (55 mM sodium citrate, 30 mM EDTA, 150 mM NaCl, 5 μM YOYO-1) was introduced into the 100 μm channel until it reaches the DNA trapping region to free the genomic DNA from the AMP. Suction was then gently applied to the port connected to the 1 μm-deep DNA extraction channel. Extended, genomic DNA is visualized in the 488 nm channel using a CCD camera (Andor, Belfast, UK).

III. RESULTS AND DISCUSSION

We validated AMP encapsulation of single, cultured, human lymphoblast cells as a sample preparation protocol for whole single cell genomes using a water-in-oil droplet generating device [Fig. 3(a)]. Consistent single-cell encapsulation was verified using both differential interference contrast (DIC) [Fig. 3(b)] and fluorescence imaging of cells labeled with SYTO dye. We determined that the average AMP diameter was 97 μm [Fig. 3(c)] for a droplet generator with a "nozzle" 100 μm in diameter. The droplet size could be modulated by tuning the nozzle diameter. In particular, we demonstrated that AMPs with diameters of less than 30 μm could be produced using a 50 μm diameter nozzle. Smaller particles hold several advantages over larger ones, including faster diffusion times for reagents, greater sample density per unit volume, and an ability to interface with other fluidic technologies, such as fluorescence-activated cell sorting (FACS). We continued our experiments with larger droplets since the smaller nozzle designs were unreliable for producing AMPs of this size homogenously and were observed to lead to particle aggregation.

We first verified in-alginate lysis using time course analysis of fluorescence imaging of trapped chromatin using the membrane-impermeable intercalator, YOYO-1. We employed a customized droplet generator which included an array of traps to stabilize the AMPs during the introduction of lysis buffer doped with YOYO-1. Microfluidic traps were designed according to a principle of dynamic hydraulic resistance as the AMPs make their way into the cavity.[28] As AMPs secured in microfluidic traps were exposed to lysis buffer, they exhibited an increase in fluorescence intensity which is consistent with the known behaviour of lipid membrane disruption (Fig. 4). The labeled DNA exhibited sufficient signal-to-noise relative to the AMP background, demonstrating the suitability of alginate-based hydrogels for fluorescence analysis. Continuous observation of the trapped AMP following the lysis event verified that the fluorescent signal remained contained within the hydrogel. As such, we concluded that the system was

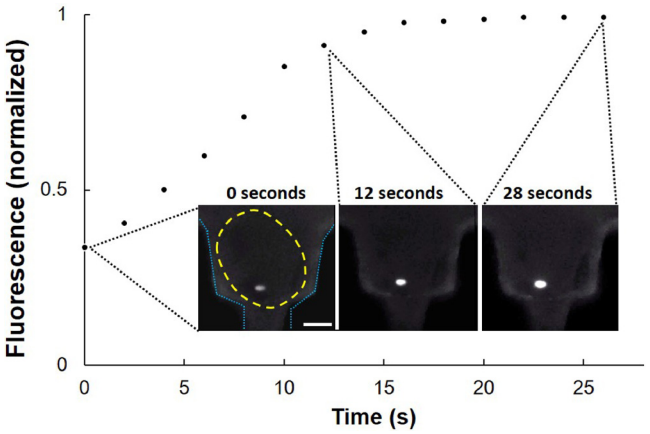

FIG. 4. Fluorescence timecourse during hydrogel droplet cell lysis of an encapsulated lymphoblast. The intensity was normalized to the brightest pixel intensity value in the field of view. Insets: A trapped AMP (yellow dashed line) with an encapsulated lymphoblast is visualized during the lysis process. Cells are initially labeled with SYTO 24 fluorescent dye, which is replaced by YOYO-1 binding to DNA after 28 s of chemical lysis. The scale bar is 100 μm.

suitable for isolating individual cells, performing cell lysis, and containing nuclear DNA. All future cell lysis was performed on the AMPs in bulk inside of an Eppendorf tube [Fig. 1(b)].

Following the bulk lysis protocol, we added a sample of AMPs to the extraction microfluidic device for isolation and release of individual genomes from the AMPs [Figs. 1(c)–1(e)]. This sample contained a mixture of both DNA-containing and empty AMPs, requiring manual selection of DNA-containing AMPs. The AMP trap was designed to stabilize selected AMPs during buffer exchange steps and facilitate the easy addition of picogram-quantity nucleic acids by pressure-driven actuation. In the future, integration of a FAC selection step will improve this bottleneck. The single-cell genomes were released from AMPs using a chelating solution according to the protocol by Tan and Takeuchi.[28] We found that chemical preparation of the cells was sufficient to remove outer lipid membranes, although nuclear protein digestion was limited considerably. Thus, when initially released from each AMP, the DNA was arranged in a tightly

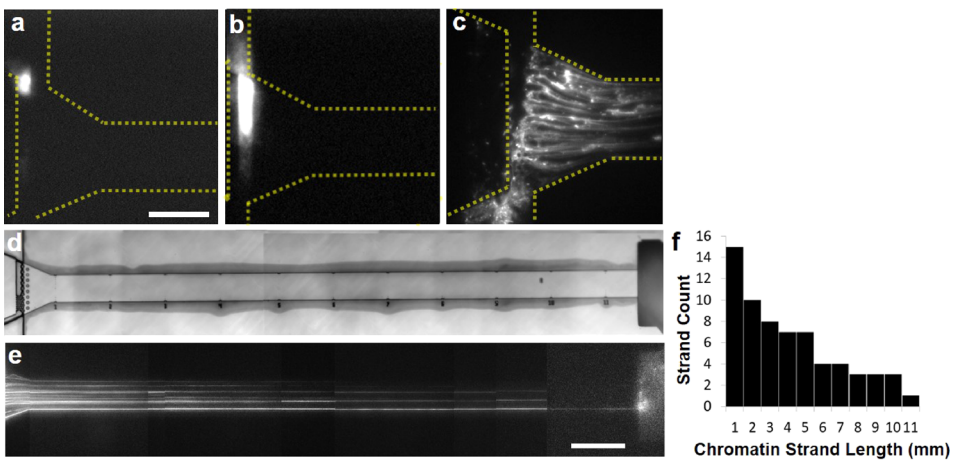

FIG. 5. Single-cell DNA loading and linearization of an individual lymphoblast genome over 11 mm. (a) Lymphoblast genomic content has been purified and introduced into the extraction junction region of the device. DNA has been labeled with YOYO-1. (b) The genomic DNA is extended near the extension region and geometrically confined near the channel entrance. (c) DNA is extracted into the extraction region using negative pressure introduced via a syringe. (d) Bright field image of the extraction region and the entire length of the extension channel. (e) The result of deliberate suction of lymphoblast nuclear DNA into the extension region of our microfluidic device. We identified several strands of high molecular weight. (f) The fragment length size was computed to determine the impact of our sample preparation technique on the population of extracted nucleic acid molecules. A histogram demonstrates the typical distribution of long DNA fragments extracted using our protocol. Scale bars are 50 μm and 1 mm.

packed conformation, necessitating the addition of fluidic shear by oscillating flow to fully extend the strands. The genomes were then introduced to a 10 μm-deep feeder channel designed to funnel directly to within 15 μm of a 1 μm-deep extension channel [Fig. 5(a)]. Lymphoblast genomes were successfully stopped at the extension channel interface by post arrays [Figs. 5(b) and 5(c)]. It is important to minimize shear stress on DNA fragments, since this will result in further fragmentation. In this manner, we attempted to minimize the pressure necessary to drive DNA closer to the extension channel, and thereby minimize the shear stress on the DNA strands at the interface of the two channels. After the DNA was stabilized, gentle suction-induced flow elongated the nucleic acids through a second post array, thereby separating individual strands. The resulting linear extension of single DNA strands within the 1 μm channel used a combination of tethered-end flow stretching and induced confinement.

The strand lengths were measured for the visible mass of extended genomic DNA inside of the 11 mm-long extension channel [Fig. 5(d)]. The longest strands spanned the entire viewing area [Fig. 5(e)]. We determined that the average strand length for the extended lymphoblast chromatin was 5 mm [Fig. 5(f)]. However, we anticipate that this result projects an incomplete picture for the extraction process due to limitations with our apparatus. We believe that our encapsulation lysis method should yield DNA strand lengths far longer than the reported 11 mm, since this result was contingent on the maximum observable strand length in the observation channel. We anticipate that lengthening the channel should resolve this limitation. Furthermore, tethered-end, flow-based stretching techniques introduce large tension and shear forces on long nucleic acid molecules and the non-equilibrium environment maintained by constant flow unravels DNA continuously towards the drainage channel. In this environment, the sampling frequency of stitching algorithms necessarily leads to an underestimation of the nucleic content for each experiment. A resolution to this limitation may be addressed through the design of serpentine channels which leave a larger amount of nucleic acid content within the field of view.[24] Finally, proximity effects near the largest DNA mass derived high intensity fluorescence and the resulting bloom disguises the number of extracted strands. While this effect is minor, we believe that it has some effect on the final proportion of extended DNA.

We report what we believe to be the longest, intact genomic DNA extracted and linearized from a single cell. We anticipate that this approach may be used in the future for performing single-molecule nucleic acid mapping on single-cells. Several techniques are compatible with microfluidic extension, including enzymatic labeling and denaturation mapping.[23] Furthermore, additional fluorescence labeling can be used to image epigenetic features layered on top of genomic data and may illuminate interplay between the two.

IV. CONCLUSION

We have demonstrated a method for handling and preparing isolated single-cells in bulk followed by delivery into a microfluidic device. We then visualized purified genomic DNA from individual cells. In addition, we found that this sample preparation protocol is effective at delivering large nucleic acids to an arbitrary microfluidic apparatus and demonstrate this by generating over 11 mm-long (33 Mbp) fragments extracted from single lymphoblasts. We demonstrated that the nucleic acid sample can be physically linearized and visualized inside of a 1 μm deep channel.

While the focus of this study was primarily on the sample preparation aspect of generating high-molecular weight, single-cell genome fragments, we envision additional assays which could be performed using this technique. Epigenetic control of gene expression occurs along large tracts of the genome, silencing or enhancing one or many genes simultaneously.[17] We envision mapping nucleosome compaction derived from histone modifications along long nucleic acids using transgenic cell lines or antibody labeling.[29] Since the impact of histones on chromatin stretching behaviour has typically been investigated using reconstituted chromatin, our technique could be used to compare these studies to a sample harvested from cell culture. Furthermore, multicolor fluorescence imaging using single stranded DNA probes, enzymatic labeling, or melting mapping could in the future be used in conjugation with our technique to perform single-cell, single-molecule genome mapping or combine these techniques with epigenetic mapping.

ACKNOWLEDGMENTS

The authors thank Huan Chu Pham Dang and Robert Sladek from the Genome Quebec Innovation Center for providing the lymphoblast cell line. This work was supported by the National Science and Research Council of Canada (NSERC) under the Collaborative Health Research Projects (CIHR) program (CIHR, CPG-127762).

[1]B. F. Brehm-stecher and E. A. Johnson, Microbiol. Mol. Biol. Rev. **68**, 538 (2004).
[2]M. Greaves and C. C. Maley, Nature **481**, 306 (2012).
[3]J. A. Magee, E. Piskounova, and S. J. Morrison, Cancer Cell **21**, 283 (2012).
[4]M. Shackleton, E. Quintana, E. R. Fearon, and S. J. Morrison, Cell **138**, 822 (2009).
[5]T. Graf and M. Stadtfeld, Cell Stem Cell **3**, 480 (2008).
[6]J. D. Lathia, J. M. Heddleston, M. Venere, and J. N. Rich, Cell Stem Cell **8**, 482 (2011).
[7]M. G. Krebs, R. L. Metcalf, L. Carter, G. Brady, F. H. Blackhall, and C. Dive, Nat. Rev. Clin. Oncol. **11**, 129 (2014).
[8]K. Sermon, A. V. Steirteghem, and I. Liebaers, The Lancet **363**, 1633 (2004).
[9]T. A. Duncombe, A. M. Tentori, and A. E. Herr, Nat. Rev. Mol. Cell Biol. **16**, 554 (2015).
[10]E. A. Ottesen, Science **314**, 1464 (2006).
[11]Y. Marcy, T. Ishoey, R. S. Lasken, T. B. Stockwell, B. P. Walenz, A. L. Halpern, K. Y. Beeson, S. M. D. Goldberg, and S. R. Quake, PLoS Genet. **3**, e155 (2007).
[12]J. Wang, H. C. Fan, B. Behr, and S. R. Quake, Cell **150**, 402 (2012).
[13]A. K. White, M. VanInsberghe, O. I. Petriv, M. Hamidi, D. Sikorski, M. A. Marra, J. Piret, S. Aparicio, and C. L. Hansen, Proc. Natl. Acad. Sci. U.S.A. **108**, 13999 (2011).
[14]Y. Xin, J. Kim, M. Ni, Y. Wei, H. Okamoto, J. Lee, C. Adler, K. Cavino, A. J. Murphy, G. D. Yancopoulos, H. C. Lin, and J. Gromada, Proc. Natl. Acad. Sci. U.S.A. **113**, 3293 (2016).
[15]N. E. Navin, Genome Biol. **15**, 452 (2014).
[16]S. Bose and P. A. Sims, "Micro- and Nanosystems for Biotechnology," in *Genome-Wide Analysis of Single Cells and the Role of Microfluidics* (2016), Vol. 29, Ch. 2.
[17]J. J. Benítez, J. Topolancik, H. C. Tian, C. B. Wallin, D. R. Latulippe, K. Szeto, P. J. Murphy, B. R. Cipriany, S. L. Levy, P. D. Soloway, and H. G. Craighead, Lab Chip **12**, 4848 (2012).
[18]Y. Xu, Q. Wu, Y. Shimatani, K. Yamaguchi, S. Azimi, Z. Dang, C. Zhang, J. Song, M. B. H. Breese, C. H. Sow, J. A. V. Kan, J. R. C. V. D. Maarel, S. M. Friedrich, C. Zec, T.-h. Wang, S. M. Friedrich, H. C. Zec, D. T. Chiu, and H. Oana, Lab Chip **14**, 8 (2014).
[19]S. Mahshid, M. J. Ahamed, D. Berard, S. Amin, R. Sladek, S. R. Leslie, and W. Reisner, Lab Chip **15**, 3013 (2015).
[20]A. Cerf, H. C. Tian, and H. G. Craighead, ACS Nano **6**, 7928 (2012).
[21]J. R. Moffitt, Y. R. Chemla, S. B. Smith, and C. Bustamante, Annu. Rev. Biochem. **77**, 205 (2008).
[22]J. W. Yeh and K. Szeto, Biomicrofluidics **11**, 044108 (2017).
[23]W. Reisner, J. N. Pedersen, and R. H. Austin, Rep. Prog. Phys. **75**, 106601 (2012).
[24]C. Freitag, C. Noble, J. Fritzsche, F. Persson, M. Reiter-Schad, A. N. Nilsson, A. Granéli, T. Ambjörnsson, K. U. Mir, and J. O. Tegenfeldt, Biomicrofluidics **9**, 044114 (2015).
[25]S. Mazzitelli, L. Capretto, F. Quinci, R. Piva, and C. Nastruzzi, Adv. Drug Delivery Rev. **65**, 1533 (2013).
[26]Z. Zhu and C. J. Yang, Acc. Chem. Res. **50**, 22 (2017).
[27]S. Bigdeli, R. O. Dettloff, C. W. Frank, R. W. Davis, and L. D. Crosby, PLoS One **10**, e0117738 (2015).
[28]W.-H. Tan and S. Takeuchi, Proc. Natl. Acad. Sci. U.S.A. **104**, 1146 (2007).
[29]S. F. Lim, A. Karpusenko, A. L. Blumers, D. E. Streng, and R. Riehn, Biomicrofluidics **7**, 064105 (2013).